Solidification of Austenitic Stainless Steel Weldments: Part III—The Effect of Solidification Behavior on Hot Cracking Susceptibility

The formation of a low-melting eutectic and S and P segregation along fusion zone grain boundaries promotes the formation of hot cracks

BY J. C. LIPPOLD AND W. F. SAVAGE

ABSTRACT. The hot cracking susceptibility of several austenitic stainless steel filler metals and a Type 304L stainless steel base metal was evaluated using the Varestraint test. Generally, alloy weldments which exhibited Ferrite Number (FN) 6-12 and solidified as primary delta ferrite were the most resistant to fusion zone hot cracking, although no direct correlation was found between FN and crack susceptibility.

Fully austenitic Type 310 and highly-ferritic Type 312 weld pads were particularly susceptible to hot cracking and exhibited extensive backfilling of fusion zone cracks. The higher alloy content of both Type 310 and Type 312 promoted the formation of a greater proportion of eutectic constituents along grain and subgrain boundaries in the fusion zone during the final stages of solidification and rendered these alloys more susceptible to hot crack formation. In addition, considerable sulfur and phosphorus segregation was detected in backfilled regions of Type 308, 310, and 312 weldments.

Introduction

Effect of Ferrite on Hot Cracking Resistance

The beneficial effects of delta ferrite in reducing or preventing hot cracking in austenitic stainless steel weldments was first reported in the early 1940's (Ref. 1). Initial work by Borland (Ref. 2) and Hull (Ref. 3) indicated that austenitic stainless steel welds and castings which contain 5-10 volume-percent delta ferrite provide optimum resistance to hot cracking in a variety of alloys. Since that time, numerous investigations concerned with the properties and weldability of fully-austenitic and duplex stainless steels in both cast and wrought form have been reported.

Hot cracking, or solidification cracking, is believed to occur at or above the solidus temperature of the lowest melting phase present (Ref. 4, 5). During the final stages of solidification, narrow, solid bridges separating areas of low melting liquid are subject to the greatest proportion of the shrinkage-induced strains. An increase in the amount of low-melting phase or in the inherent strain resulting from solidification shrinkage may cause fracture of these solid bridges, thus forming hot cracks.

Investigations of fully-austenitic weld metals have revealed a high incidence of hot cracking both in the fusion zone and in the base metal adjacent to the fusion zone. The cracking susceptibility of these steels is attributed to the presence of low-melting films along grain and subgrain boundaries (Ref. 6-8). Microprobe analysis of the intergranular regions indicated that these low-melting films were enriched in elements such as sulfur, phosphorus, silicon, and manganese (Ref. 7, 9-11). Work performed by Cordea et al. (Ref. 6) on ultra-pure Type 310 indicated that a decrease in solidification cracking occurred as a result of reducing sulfur and phosphorus levels to trace amounts. Reducing the silicon content to less than 0.10 wt-% was found to be helpful in preventing the formation of continuous liquid films along austenite boundaries.

In addition to the cracking associated with eutectic and other low-melting films, several investigators have reported the incidence of what is termed "ductility-dip" cracking (Ref. 6, 9, 12). Such cracking propagates intergranularly in the solid state at temperatures 100–300°C (200–600°F) below the equilibrium solidus, and the cracks formed are generally much less extensive than solidification cracks. The incidence of both heat-affected zone (HAZ) cracking (Ref. 13) and cracking in previous passes of multipass welds (Ref. 14) have also been reported in fully-austenitic weldments.

By comparison, austenitic stainless steels which produce a duplex austenite-ferrite microstructure in as-deposited welds are reported to be more resistant to both fusion zone and HAZ hot cracking than fully-austenitic alloys. It is proposed that the greater grain boundary area present in duplex weldments reduces the chances of forming continuous low-melting films along grain boundaries (Ref. 2). In addition, the fact that delta ferrite has a greater solubility for harmful elements such as sulfur and phosphorus than does austenite is postulated to reduce the volume of low-melting constituents formed during solidification (Ref. 2, 3, 6, 8, 9).

The relative hot cracking susceptibility of austenitic stainless steels has been compared by a variety of methods including the cast pin tear test (Ref. 3), the Varestraint test (Ref. 8,12,15), the fissure bend test (Ref. 14), and several others (Ref. 7,10,16,17). Regardless of the testing method used, the conclusion reached is that welds containing a few volume-percent delta ferrite at room temperature are generally more resistant to hot cracking than fully-austenitic welds. Results of such tests indicate that, although fusion zone and HAZ cracks may be present in duplex weldments, they are less severe than those found in fully-austenitic welds.

Effect of Alloy Composition on Ferrite Distribution and Morphology

The distribution and morphology of delta ferrite in austenitic stainless steel

J. C. LIPPOLD, a former Graduate Fellow at Rensselaer Polytechnic Institute, is with Sandia National Laboratories, Livermore, California; W. F. SAVAGE is Professor of Metallurgical Engineering and Director of Welding Research, Rensselaer Polytechnic Institute, Troy, New York.

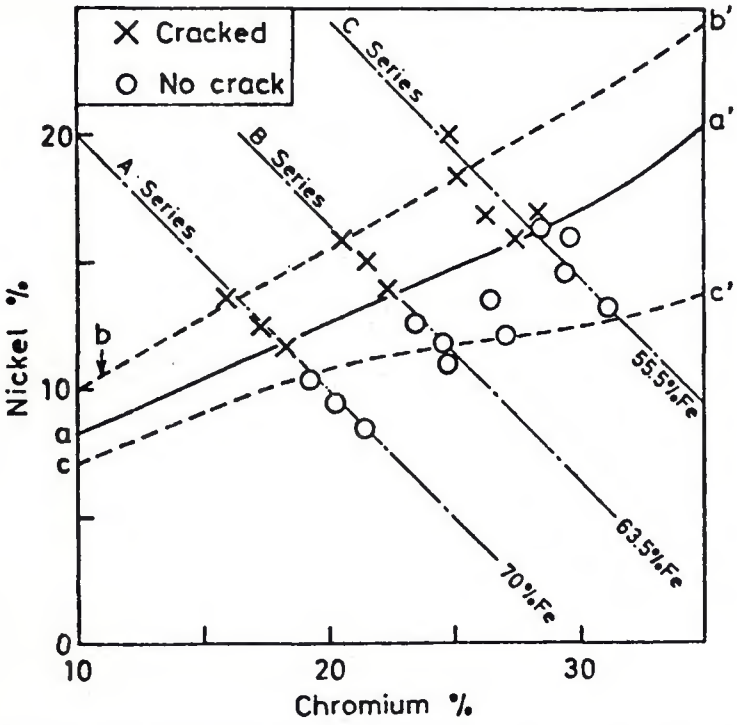

Fig. 1 — Crack sensitivity of alloys relative to the Fe-Cr-Ni ternary system (from Masumoto et al. — Ref. 16)

weldments is dependent on the electrode and base metal compositions, welding parameters, the local weld cooling rate, and the degree of dilution. Recognizing that the chemical composition has the greatest effect on controlling the amount of retained ferrite, Schaeffler (Ref. 18) and more recently DeLong (Ref. 19) have developed diagrams for predicting the volume-percent of weld metal ferrite.

Attempts to reduce hot cracking susceptibility in fully austenitic weldments by varying the alloy composition has met with limited success. Although many authors have reported that reducing the sulfur and phosphorus content increases the hot cracking resistance (Ref. 2, 7, 9-11), reduction of these elements to trace amounts in both base materials and filler metals is difficult and costly. Increasing manganese contents from normal levels (generally 1-2 wt-%) to 5-10% decreases hot cracking resistance as a result of its ability to combine with excess sulfur. However, there is some indication that increased manganese results in decreased corrosion resistance (Ref. 20).

Extensive studies by Hull (Ref. 21) and others (Ref. 9-11, 15, 20, 22) reported the harmful effects of silicon, columbium, and titanium on hot cracking resistance. An increase in the carbon content from 0.1 to 0.4-0.5 wt-% reduced the extent of microfissuring by increasing the amount of interdendritic eutectic available to backfill cracks formed at high temperatures (Ref. 9). However, high carbon contents promote sensitization and subsequently degrade corrosion resistance.

Results of hot cracking tests performed by Arata et al. (Ref. 15) indicate that small additions of nitrogen to the shielding gas can significantly reduce the amount of retained delta ferrite and result in an increase in hot cracking. The effect of nitrogen is particularly important since increasing the arc length during welding increases the nitrogen content of the as-deposited weld metal (Ref. 23).

Although weld metal composition is important in determining the amount of ferrite present in an as-deposited weld, welding parameters influence both the cooling rate and dilution and thus significantly affect both the amount and the morphology of the ferrite (Ref. 24). High heat input welds result in slow cooling rates and thus coarse microstructures, although studies performed by Watanabe et al. (Ref. 23) indicate that heat input has little effect on the overall ferrite content if dilution effects are neglected. However, control of both weld dilution and arc length through proper selection of welding parameters is necessary to maintain desired levels of delta ferrite in the resultant weldment.

Microsegregation During Solidification

The microsegregation which results from non-equilibrium weld solidification has been rigorously reviewed in both Part 1 and Part 2 of this investigation (published December, 1979, and February, 1980, respectively, in the *Welding Journal*). Solidification under Case III solidification conditions* results in local compositional variations of chromium and nickel within the weld substructure. In addition, the segregation of secondary alloying elements to grain and subgrain boundaries during solidification may occur to varying degrees with a subsequent effect on the hot cracking susceptibility of the weldment.

During solidification as primary austenite, chromium, silicon, sulfur, and phosphorus are rejected to the liquid and may exist in relatively high concentrations in the final solid which forms along the solidification boundaries. Matsuda et al. (Ref. 25) observed particularly high levels of phosphorous along cell boundaries in fully austenitic weldments and related this to the inferior weldability of these alloys.

During solidification as primary delta ferrite, relatively less sulfur and phosphorus is rejected to the liquid. In addition, the last-to-solidify region is enriched in both manganese and silicon, and thus these elements are more likely to combine to form phosphides and sulfides (Ref. 9). Carbon was not found to segregate significantly during primary gamma or delta solidification.

The importance of primary solidification from the liquid was illustrated by hot cracking tests performed by Masumoto et al. (Ref. 16). Fusion welds which solidified as primary austenite were susceptible to hot cracking, while those which formed primary delta ferrite were immune. Figure 1 shows the relative position of these alloys with respect to the Fe-Cr-Ni ternary phase diagram. Clearly, this work indicates that control of the solidification mode is important in producing crack-free welds and castings. In addition, the authors found no correlation between cracking susceptibility and the ferrite content as estimated by the Schaeffler-DeLong diagram. This is an extremely significant indictment against the concept of correlating the ferrite content at room temperature with the susceptibility to hot cracking.

Objectives

The objectives of this portion of the investigation were:

1. To evaluate the hot cracking susceptibility of a full range of austenitic stainless steel filler metals and a Type 304L base material which solidify as either primary austenite or primary ferrite.
2. To determine the relationship between the solidification process and the hot cracking propensity of these alloys.

**In Case III solidification there is no diffusion in the solid and no mechanical mixing in the liquid. Concentration changes in the liquid occur by diffusion only. These boundary conditions can be shown to be closely approximated in most fusion welding processes.*

Table 1—Chemical Composition Wt-%[a]

Material	Cr	Ni	Si	Mn	Mo	C	S	P
304L (base metal)	18.65	9.66	0.64	1.57	–	0.024	0.011	0.034
316	18.80	12.16	0.48	1.72	2.28	0.067	0.017	0.029
V-308	20.07	10.08	0.41	1.02	0.09	0.045	0.023	0.015
308	20.42	9.92	0.31	1.84	0.14	0.050	0.019	0.025
309	23.60	12.32	0.44	1.62	–	0.070	0.008	0.014
312	29.44	8.79	0.44	1.61	0.21	0.120	0.013	0.020
310	27.11	21.50	0.47	1.65	0.07	0.110	0.002	0.014

[a]Average of two independent analyses

Table 2—Welding Parameters for Varestraint Specimen Preparation and Testing

Specimen preparation	
Welding process:	Gas metal arc (GMA), three passes
Arc current:	200 ± 10 A
Arc voltage:	28 ± 1 V DCRP
Filler metal feed rate:	375 ipm (159 mm/s)
Carriage travel speed:	12.5 ipm (5 mm/s)
Shielding gas:	Argon-2% O_2, 40 cfh
Varestraint testing	
Welding process:	Gas tungsten arc (GTA)
Arc current:	180 ± 10 A
Arc voltage:	12 ± 0.5 V, DCSP
Travel speed:	4 ipm (1.7 mm/s)
Shielding gas:	Argon, 40 cfh
Electrode-work distance:	3/32 in. (2.4 mm), measured cold
Electrode:	1/8 in. (3.2 mm), centerless ground, W-ThO_2
Electrode extension:	1.5 in. (38.1 mm) from the water-cooled collet

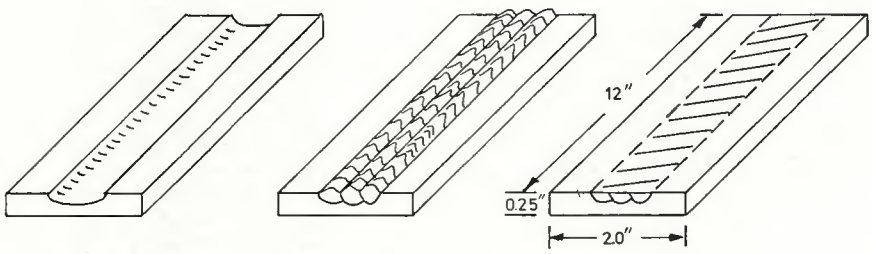

Fig. 2—Schematic of Varestraint sample preparation

Experimental Procedure

The hot cracking susceptibility of a full range of commercial austenitic stainless steel filler metals was evaluated using the Varestraint test (Ref. 26). These included filler metals which produced either fully-austenitic or duplex microstructures in the as-welded condition. In addition, a Type 304L base material was tested. The compositions of these alloys are listed in Table 1.

Varestraint specimens were prepared in the following manner. A 6.4 mm (¼ in.) thick Type 304L stainless steel plate was selected for the base material. The plate was sectioned into bars of dimensions of 0.64 × 5.1 × 30.5 (¼ × 2 × 12 in.). A groove 0.2 cm (0.080 in.) deep and 16 mm (0.615 in.) wide was then machined parallel to the 30.5 cm (12 in.) dimension along the centerline of the 5.1 cm (2 in.) dimension. The bars were thoroughly degreased with acetone and wiped dry.

Three gas metal arc (GMA) welds were deposited in the groove using the desired filler metal to produce a single layer weld deposit. The welding parameters used are listed in Table 2. Individual welds were wired, brushed and thoroughly cleaned between passes. Following welding, the weld reinforcement was machined flush with the specimen surface and the surface was belt sanded to remove any oxides formed during the GMAW process. The specimens were again degreased with acetone prior to Varestraint testing. The three-step sample preparation is illustrated schematically in Fig. 2.

Specimens were tested over a range of augmented strains from ¼ to 2%, giving results shown in Table 3. Following testing, the extent of hot cracking in each sample was determined with the aid of a binocular microscope equipped with a filar eyepiece. A magnification of ×50 was used to measure crack lengths. For each sample the total crack length, maximum crack length, and total number of cracks was recorded. A distinction was made between fusion zone cracks and

Table 3—Results of Testing at Augmented Strains of 1% and 2%

Material	Relative hot-cracking resistance	Average crack length, in.[a]	Total crack length, in.[b]	Ferrite Number	
				Magne Gage	DeLong[c]
304L (base metal)	1	0.006	0.032	5.5	5.0
309	2	0.008	0.047	10.5	11.5
316	3	0.008	0.060	6.5	5.0
V-308	4	0.010	0.089	10.0	9.0
308	5	0.011	0.112	9.0	8.0
312	6	0.019	0.193	> 40	–
310	7	0.027	0.318	< 1.0	–

[a]Determined at 2% augmented strain.
[b]Determined at 1% augmented strain.
[c]Weld pad dilution by Type 304L base metal estimated to be 30%.

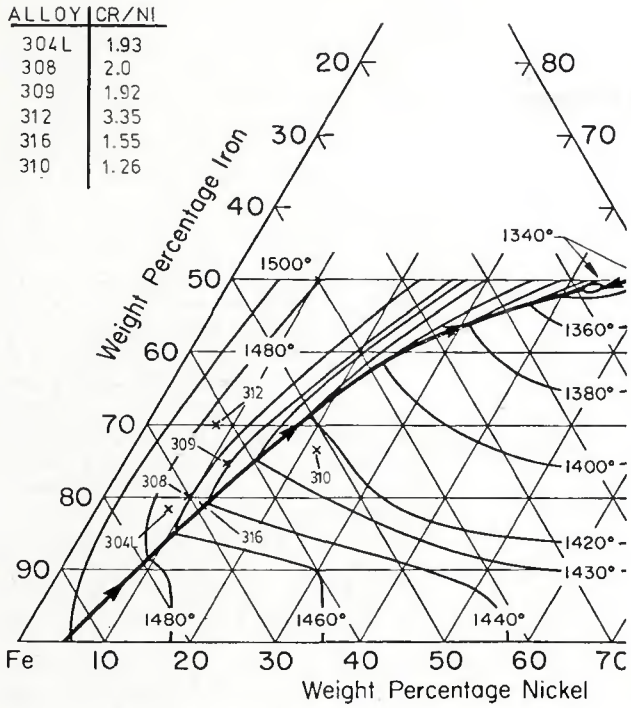

Fig. 3 — Location of commercial 300-series alloys relative to the Fe-Cr-Ni liquidus surface

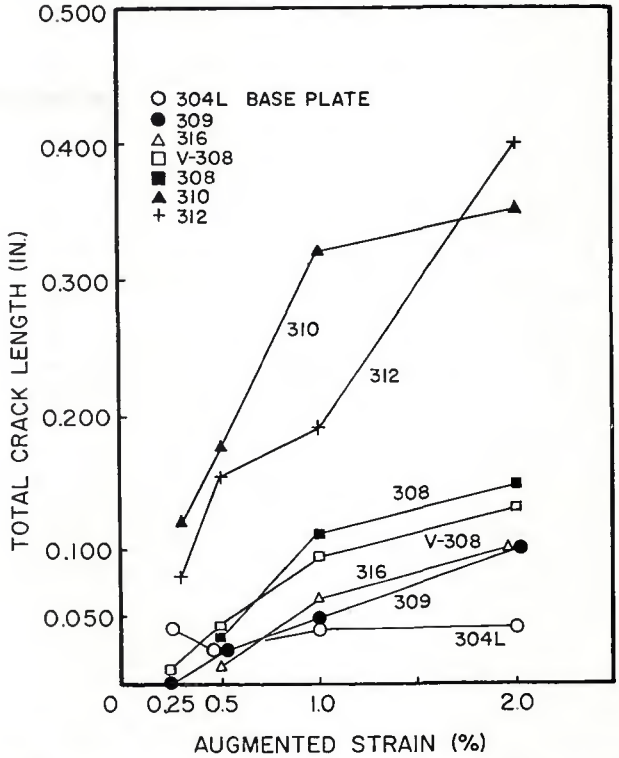

Fig. 4 — Total crack length vs. augmented strain for 300-series filler metals and a Type 304L base metal tested using the Varestraint test

fissures associated with the HAZ.

The ferrite number (FN) of the weld pad was determined prior to testing using the Magne Gage. Three readings were taken at 25 mm (1 in.) intervals along the pad. In addition, the FN of the sample was measured following Varestraint testing. The DeLong diagram (Ref. 19) was also employed to estimate weld metal ferrite content.

Microanalysis of selected areas of the Varestraint specimens was performed with the aid of the electron microprobe at an accelerating voltage of 20 kV with a nominal specimen current of 0.25 microamperes. The spatial resolution of the electron probe was on the order of 2–3 microns.

Results and Discussion

Solidification Behavior

In order to predict the initial solidification product of the Type 304L base material and the filler metal weld pads which were evaluated with the Varestraint test, the position of these alloys relative to the Fe-Cr-Ni liquidus surface is illustrated in Fig. 3. Since dilution of the filler metal by the base material during specimen preparation was on the order of 30%, the final composition of the alloy weld pads was shifted along a tie line connecting the individual filler metal composition to that of the Type 304L base metal.

Since the Cr/Ni ratio of Types 304L, 308 and 309 are roughly equivalent and that of Type 312 is considerably higher, dilution by the Type 304L base metal had no effect on the initial solidification product; in all weldments made with these alloys, delta ferrite was the primary phase formed during solidification. The composition of Type 316 lies on the line separating the Cr-rich primary delta ferrite region from the Ni-rich primary austenite region; thus, dilution of this alloy by the base metal increased the ultimate Cr/Ni ratio and favored solidification as primary delta ferrite.

By contrast, despite dilution of the Type 310 filler metal by the base metal the final weld pad composition remained within the Ni-rich region where solidification occurs as primary austenite. In addition, the austenite-stabilizing effect of the nominal carbon and nitrogen concentrations in the weld pad was not sufficient to shift the primary phase from that predicted by Fig. 3.

Evaluation of Hot Cracking Susceptibility

The best index of relative hot cracking susceptibility among the filler metals was provided by plotting the total crack length, measured on the surface of the as-welded pad, versus the augmented strain, over a range from ¼ to 2%, as illustrated in Fig. 4. Using this method, Type 310 and Type 312 weld metal pads proved to be more susceptible to fusion zone hot cracking over the full range of augmented strain than any of the other commercial weld pads or the autogenous welds on the Type 304L base metal. Cracking associated with the heat-affected zone (HAZ) was generally insignificant and is not included in the data presented in Fig. 4.

At 2% restraint, Type 304L exhibited only half the total crack length of both Type 316 and 309, which in turn were more resistant to hot cracking than either lot of Type 308. In addition, Type 310 and 312 weld pads exhibited over three times the total crack length of the other alloys at the same restraint level.

Comparison of the maximum crack length at various strains within the same alloy composition or among different alloys at equivalent strains proved to be a poor index for evaluating relative hot cracking resistance. Frequently, one large crack in the as-tested weld pad would be accompanied by several small fissures and thus would not be representative of the overall behavior of the pad. The threshold strain, or limiting strain at which materials are determined to be crack resistant, was more indicative of the hot cracking resistance of the alloys. Type 316 proved to be effectively crack resistant at 0.5% strain, while Types 308, 309

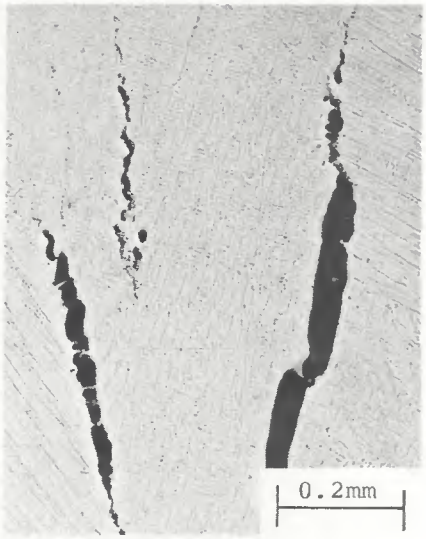

Fig. 5—Hot cracks in a Type 310 weld pad tested at 2% restraint. Mixed acid etch. ×100 (reduced 17% on reproduction)

and 304L exhibited a similar degree of crack resistance at 0.25%. Types 310 and 312 were susceptible to hot cracking at 0.25%, and thus the threshold strain for these alloys lies below this value of augmented strain.

The determination of the average crack length among alloys tested at equivalent augmented strain provided another suitable method for evaluating relative hot cracking resistance from the Varestraint crack length data. Both the average crack length, evaluated at 2% restraint, and the total crack length, from the alloy pads and autogenous Type 304 base metal tested at 1% restraint, are listed in Table 3.

Based on these two criterion Type 304L was the most crack resistant, while Types 310 and 312 again proved to be the most susceptible to weld hot cracking.

Similar results were obtained by Lundin (Ref. 27), who employed the fissure bend test and Arata et al. (Ref. 15) who utilized the Varestraint test. In general, they found that alloys which solidified as primary austenite and, as a consequence, exhibited little or no retained ferrite in the weld deposit were more susceptible to hot cracking.

Relation of Crack Resistance to Ferrite Number

The ferrite numbers (FN) of the weld metal pads, determined with the aid of both the Magne Gage and the DeLong diagram are also listed in Table 3. Their listing was an attempt to correlate the amount of weld metal ferrite with the resistance to hot cracking. Since little change in the overall FN occurred as a result of the GTA weld pass employed during the Varestraint test, Magne Gage readings taken prior to testing are presented. The FN as estimated by the DeLong diagram was adjusted for the dilution of the filler metals by the Type 304L base metal, although the limited range of the diagram precluded estimation of weld metal ferrite in the highly-alloyed Type 310 and Type 312 weld pads.

Despite the difference in ferrite measurement methods, the DeLong diagram and the Magne Gage provided comparable estimates of weld metal ferrite. In addition, a rough correlation existed between the apparent FN of the weld pad and its corresponding resistance to hot cracking. The Type 310 weld pad which solidified as primary austenite and contained essentially no delta ferrite (FN < 1) was extremely susceptible to hot cracking, while Types 316, 308 and 309, which solidified as primary delta ferrite and exhibited FN 6-12, proved to be more crack-resistant. However, the Type 304L base material which solidified as primary delta ferrite exhibited the best resistance to hot cracking. This occurred despite the fact that the as-tested weldment exhibited only FN 5, while the Type 312 weld pads which exhibited a FN 40 were extremely susceptible to cracking.

It is apparent that alloys which by nature of their initial composition exhibit either a minimal amount of retained ferrite such as Type 310, or an extreme amount such as Type 312, are inherently susceptible to hot cracking. On the other hand, there appears to be no direct correlation of the FN with the cracking susceptibility of the alloys which fall between these two extremes. For example, Type 308 with FN 12 is more susceptible than Type 304L with FN 5 at an equivalent level of restraint. It is interesting to note, however, that a correlation does exist between the sulfur content of these alloys (304L, 308, 316, and 309), as listed in Table 1, and the cracking susceptibility presented in Table 3. Both Type 304L and Type 309 which contain relatively low levels of sulfur are more crack resistant than both heats of Type 308 and also Type 316 which contain increased levels of impurity elements.

Thus, the amount of residual delta ferrite necessary to ensure an "acceptable" level of hot cracking resistance is specific to a particular alloy composition, and, unfortunately, may vary greatly within the nominal composition limits of that alloy (Ref. 28).

Microstructure of the Varestraint Weld Pads

Metallographic examination of the various alloy weld pads revealed that hot cracks propagate primarily along fusion zone grain boundaries (as defined by changes in substructure growth orientation) irrespective of the solidification behavior of the particular alloy. Fully austenitic Type 310 weld pads exhibited large austenite grains, which provided smooth paths for the initiation and propagation of hot cracks. The extreme degree of macrocracking, which occurred at these sites when this alloy was tested at 2% restraint, is evident in Fig. 5. In addition, numerous fissures were

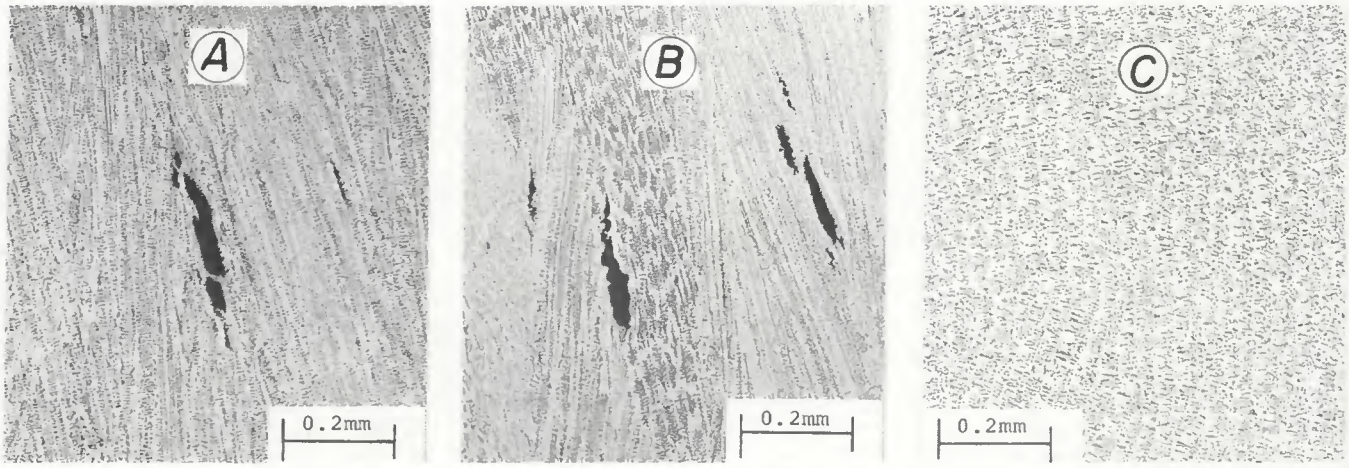

Fig. 6—Hot cracks in weld pads tested at 2% restraint: A—Type 316; B—Type 308; C—Type 309. Mixed acid etch. ×100 (reduced 26% on reproduction)

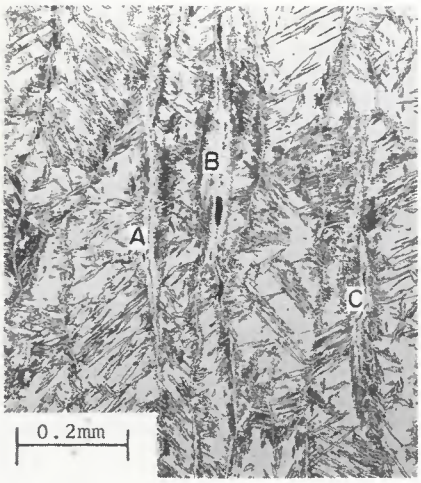

Fig. 7—Hot cracks in Type 312 weld pad tested at 2% restraint. Note backfilling at A, B and C. Mixed acid etch. ×100 (reduced 28% on reproduction)

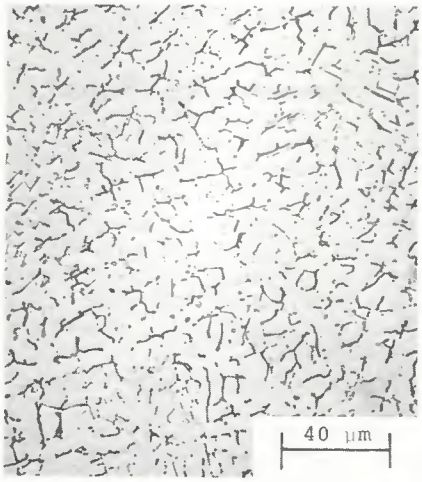

Fig. 8—Fusion zone microstructure of Type 304L weld pad. Mixed acid etch. ×500 (reduced 28% on reproduction)

observed; these initiated and propagated in the solid-state, remote from the solid-liquid interface at the instant of applied strain. The "ductility-dip" cracks have been observed by previous investigators (Ref. 9, 15, 16) in fully austenitic weldments (these were not included in the crack length data of Fig. 4).

The alloy weld pads, which solidified as primary delta ferrite and contained less than FN 12 in the as-deposited weld pad, exhibited a more refined microstructure and were typically more resistant to weld hot cracking than the fully austenitic weldments. Weld pads produced with Types 316, 308 and 309 filler metals and tested at 2% restraint are shown in Fig. 6.

The duplex microstructure in these alloy pads is characterized by a vermicular distribution of dark-etching delta ferrite separated by the unetched austenite. Both Type 308 and Type 316 exhibited small cracks along fusion zone grain boundaries, although no cracks were observed in the Type 309 weld pad following mechanical polishing. In addition, ductility-dip cracks were not observed in any of the duplex stainless steel weld pads which were tested.

Alloy pads produced with Type 312 filler metal solidified initially as primary delta ferrite but upon cooling to room temperature precipitation of Widmanstätten austenite occurred along the ferrite grain and subgrain boundaries. The resultant microstructure consisted of large ferrite grains surrounded by a continuous austenite phase at the grain boundaries, as shown in Fig. 7. It is these continuous austenite networks which provide sites for the initiation and propagation of hot cracks during the Varestraint tests. In addition to the "open-crack" morphology shown previously, significant grain boundary liquation and crack backfilling was observed in Type 312 Varestraint specimens, as may be seen at points A, B, and C in Fig. 7.

Hot cracking was observed in both the fusion zone and adjacent HAZ of the Type 304L Varestraint specimens. Although some small cracks were observed during crack length measurements on the as-welded surface, all disappeared after mechanical polishing. Therefore, no photomicrographs of cracks in Type 304L could be obtained. However, the resultant fusion zone microstructure which exhibits a vermicular ferrite morphology (FN 5) is shown in Fig. 8.

It is postulated that superficial hot cracks in the HAZ of the 304L base metal initiated along liquidated austenite grain boundaries or solute bands and propagated into the fusion zone upon application of sufficient augmented strain. However, the cracks were either very shallow or were healed by backfilling except at the surface of the weldment.

Morphology of Fusion Zone Hot Cracks

Frequently, regions near the boundaries and tip of the fusion zone cracks appeared metallographically distinct from adjacent regions in the bulk microstructure. Their appearance suggested that crack backfilling by liquid of dissimilar composition may occur during the final stages of solidification. Since the composition of this backfilled material is either enriched or depleted in solute (depending on the particular distribution coefficient, k_o, of the solute element), the effective solidus temperature of this material is depressed below that of the bulk solidus and subsequently promotes the formation of hot cracks in the presence of sufficient mechanical and/or shrinkage strains.

Figure 9 provides a schematic representation of the situation which exists at the advancing solid-liquid interface at the instant that strain is applied during the Varestraint test. Note that a narrow region of solute enrichment or depletion exists within the liquid slightly in advance of the interface. This is representative of the steady-state stage of Case III solidification which has been reviewed previously (Ref. 29) on a microscopic scale during solidification of the individual cells or dendrites. However, since on a macroscopic scale the advancing interface is essentially planar, a liquid diffusion zone must exist between the bulk solid of nominal composition and the liquid weld pool of the same composition.

If the weldment solidifies as primary delta ferrite, the liquid diffusion zone in Fig. 9 is enriched in nickel and depleted in chromium. Conversely, during solidification as primary austenite, the region in advance of the solid-liquid interface is enriched in chromium and may be slightly depleted in nickel ($k_{Ni} \approx 1.0$).

When sufficient strain exists in the system (in this case, when the specimen is bent in the Varestraint test), cracks may form along regions where segregation tends to be the most extensive—in this case at the grain boundaries. Subsequently, solute-rich or solute-lean liquid from the diffusion zone may be drawn into the cracks by capillary action. The volume of this material tends to be great in comparison to the thin films normally encountered along subgrain boundaries (resulting from the terminal transient stage of solidification). As a result, these sites provide a unique opportunity to evaluate the composition of the last-to-solidify material often associated with the initiation and propagation of hot cracks.

Type 308. Figure 10 shows the region surrounding the crack tip at a fusion zone grain boundary in a Type 308 Varestraint weld pad tested at 2% augmented strain. Note the extensive light-etching region surrounding, and to the right of, the crack in the left hand portion of the photomicrograph; this reflects the Ni-enriched solute diffusion zone which existed in advance of the moving solid-liquid inter-

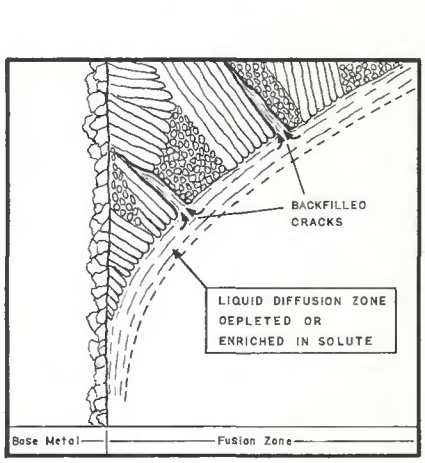

Fig. 9—Schematic showing formation of backfilled cracks

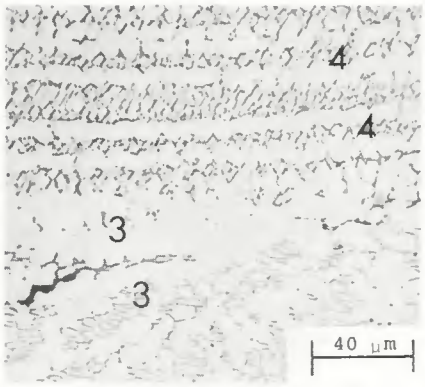

Fig. 10—Backfilled crack in Type 308 weld pad. Mixed acid etch. X500 (reduced 34% on reproduction)

face at the instant the crack formed and was drawn into the newly formed crack by capillary action. As a result, the austenite and ferrite in this region form a more extensive divorced eutectic than is normally observed and a significant amount of ferrite solidifies at the boundary (along the center line of the crack path).

A concentration profile across region 3-3 is presented in Fig. 11. This reveals that the unetched region surrounding the crack is Ni-enriched and Cr-depleted relative to the alloy nominal composition; it thus reflects the average composition of the solute diffusion zones which impinge at the boundary and backfill the resultant crack. The dark-etching material at the crack tip is enriched in chromium and, therefore, reflects the composition of the eutectic ferrite which forms during the terminal transient stage. In regions outside the boundaries of the backfilled crack, the composition rapidly approaches the nominal composition of the alloy. This reflects the steady-state solidification stage that preceded the completion of solidification. Careful analysis of the backfilled region also indicated that there exists a localized enrichment in both sulfur and phosphorus at the crack tip.

A more conventional duplex microstructure was observed in regions more remote from the fusion zone grain boundary. An acicular, austenite-ferrite morphology can be seen at region 4-4 in Fig. 10. A concentration profile across this region is presented in Fig. 12 and indicates that little variation from the nominal composition is resolvable within the acicular region. The light-etching material at the boundaries of the acicular region is accompanied by a significant enrichment in nickel and thus corresponds to the terminal transient stage of solidification. Note that no eutectic ferrite is evident within this light-etching region.

Type 312. Numerous backfilled hot cracks at fusion zone grain boundaries were observed in Type 312 weld pads which were tested at 2% restraint. A typical region in an as-tested pad is shown in Fig. 13; it is clear that the cracks propagate within fully austenitic regions of the subgrain boundaries.

Since Type 312 exhibits a high Cr/Ni ratio, this alloy solidifies as primary delta ferrite and the resultant solute diffusion zone which forms at the advancing solid-liquid interface during steady-state solidification is enriched in nickel and depleted in chromium. Thus, at the completion of solidification, as adjacent solute diffusion zones impinge, a Ni-enriched liquid backfills cracks along the grain boundaries and forms a divorced ferrite-austenite eutectic mixture in this region. Since a substantial volume of backfilled liquid exists along these boundaries a significant amount of the final solid consists of eutectic ferrite, as indicated by the arrows in Fig. 13.

Following solidification, some of the primary ferrite transforms to Widmanstätten austenite by means of a diffusion-controlled reaction as the alloy cools through the two-phase ferrite plus austenite field. This plate-like austenite, which is evident in Fig. 13, nucleates from the eutectic austenite that formed during the terminal transient stage of solidification.

Figure 14 is a concentration profile across a backfilled subgrain boundary at

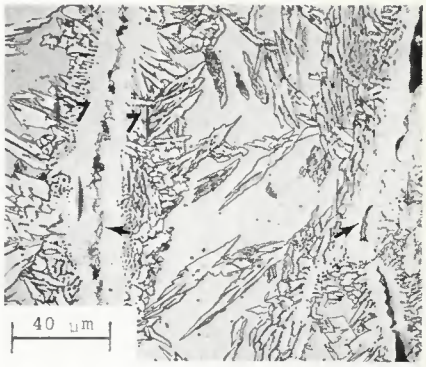

Fig. 13—Backfilled hot cracks in Type 312 weld pad. Arrows indicate eutectic ferrite particles along centerline of the backfilled region. Mixed acid etch. X500 (reduced 37% on reproduction)

position 7-7 in Fig. 13. Since a significant amount of eutectic ferrite was formed along the backfilled crack, the spatial resolution of the electron beam was improved relative to the width of this constituent. Consequently, a considerable enrichment in chromium above that of the nominal composition is observed when the beam is centered precisely on the eutectic ferrite. In addition, the region surrounding this ferrite is enriched in nickel and depleted in chromium; it corresponds to the average composition of the diffusion zone liquid which backfilled the subgrain boundary.

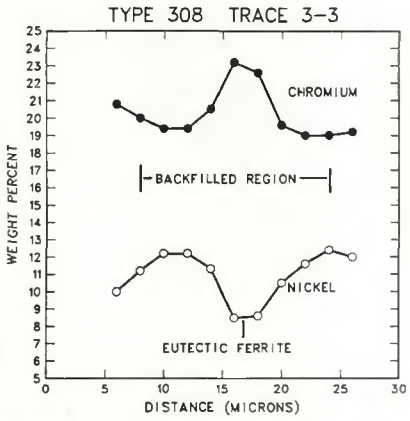

Fig. 11—Concentration profile across region 3-3 in Fig. 10

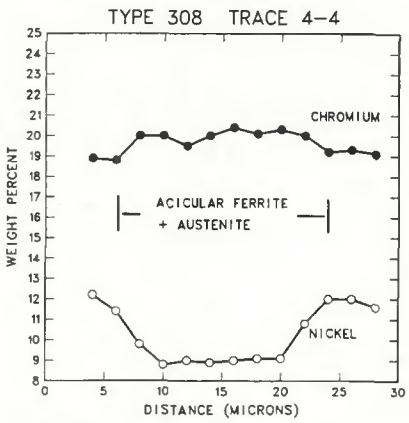

Fig. 12—Concentration profile across region 4-4 in Fig. 10

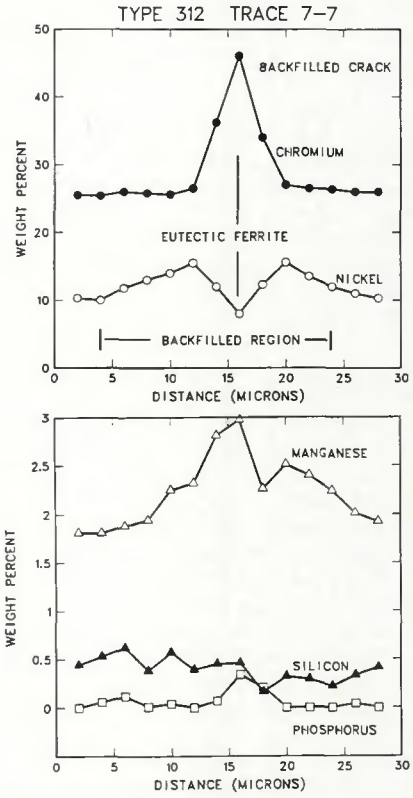

Fig. 14—Concentration profile across region 7-7 in Fig. 13

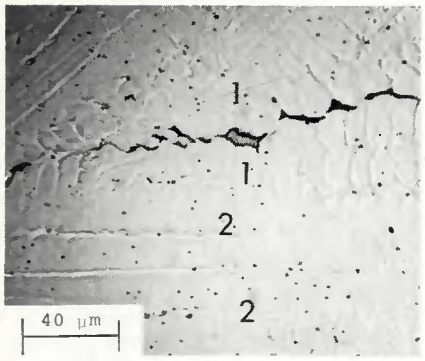

Fig. 15 — Backfilled crack region in Type 310 weld pad. Mixed acid etch. X500 (reduced 37% on reproduction)

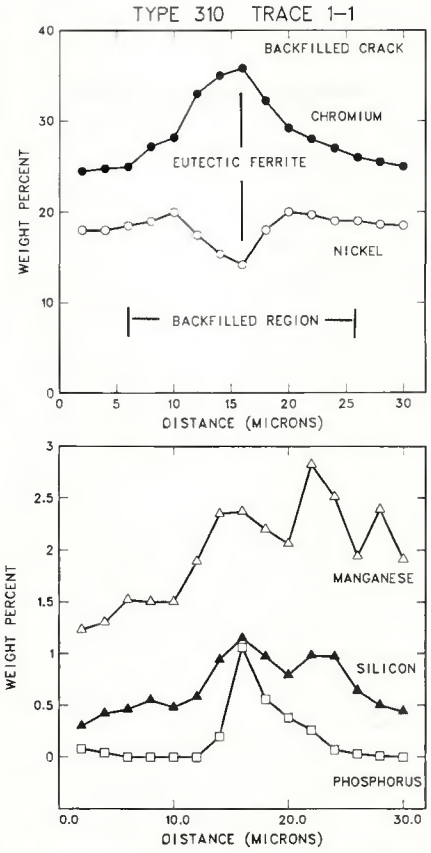

Fig. 16 — Concentration profile region across region 1-1 in Fig. 15

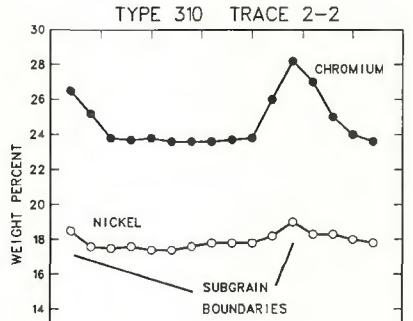

Fig. 17 — Concentration profile across region 2-2 in Fig. 15

The width of the backfilled region also permitted more accurate analysis of the silicon, manganese, and phosphorus concentrations in the last-to-solidify constituents. Sulfur analysis is confounded by the presence of molybdenum which has a characteristic x-ray peak which overlaps the $S_{k\alpha}$ peak. As a result, the degree of sulfur segregation can only be determined qualitatively at best and thus is omitted from the plot in Fig. 14.

The microprobe data for the other elements indicate that an enrichment in both phosphorus and manganese is associated with the backfilled region, while silicon exhibits little or no partitioning. A significant increase in the S(Mo) concentration was also observed; this is thought to reflect the segregation of sulfur rather than molybdenum which is a ferrite stabilizing element and would be more soluble in the ferrite during primary solidification.

Type 310. Of the alloys tested using the Varestraint test, Type 310 weld pads were unique in that solidification occurred as primary austenite. As a consequence, they contained very little delta ferrite in the as-welded microstructure. During the steady-state stage of primary austenite solidification, the diffusion zone liquid in advance of the solid-liquid interface is enriched in chromium. Thus, when this region impinges upon an adjacent diffusion layer during the terminal transient stage, a liquid persists at the grain and subgrain boundaries whose average composition is Cr-rich relative to the nominal composition. If the Cr/Ni ratio in this final liquid is sufficiently high, ferrite may form as a result of the austenite-ferrite eutectic reaction.

Numerous backfilled hot cracks were observed in Type 310 Varestraint specimens which were tested at 2% restraint. As noted previously in both Type 308 and 312 weld pads, a dark-etching constituent was frequently observed at the grain and subgrain boundaries where significant backfilling occurred, as shown in Fig. 15 at region 1-1. In addition, a definite substructure differing from that in the adjacent fusion zone subgrain is apparent on either side of the crack. This substructure is formed during the solidification of the backfilled, diffusion zone liquid contained within the already-solidified walls of the crack.

A concentration profile across the backfilled region at 1-1 is presented in Fig. 16. The profile indicates that the dark-etching constituent in the center of the backfilled crack exhibits a high Cr/Ni ratio, and hence, corresponds to the eutectic ferrite formed during the terminal transient stage of solidification. The backfilled material surrounding this constituent is enriched in chromium relative to the nominal composition and thus reflects the average composition of the steady-state diffusion zone. A substantial increase in phosphorus corresponding to the location of the eutectic ferrite indicates that the partitioning of this element is particularly severe when solidification occurs as primary austenite. The enrichment of S(Mo) in this region was small relative to the backfilled cracks in both the 308 and 312 weld pads; this was probably a result of the low concentration of these elements in the original alloy (Table 1). However, some segregation of sulfur is apparent in the backfilled region.

A concentration profile across a cellular dendrite adjacent to the backfilled grain boundary is shown in Fig. 17. The concentrations of chromium and nickel within the dendrite show little variation from the alloy nominal composition, and undoubtedly correspond to the composition of material formed during the steady-state stage of solidification. A substantial increase in chromium at the cellular dendrite boundaries is indicative of the impingement of adjacent Cr-rich diffusion layers during the terminal transient stage. Note that only scattered particles of ferrite exist along these subgrain boundaries in Fig. 15.

Relationship Between Solidification Behavior and Hot Cracking Susceptibility

Microanalysis of backfilled cracks in the austenitic stainless steel weld pads indicated that substantial regions of low-melting liquid may exist along solidification boundaries, particularly in alloys which contain a large proportion of chromium and/or nickel (such as Type 310 and Type 312). These alloys lie in closer proximity to the ternary eutectic point (49Cr-43Ni-8Fe) and would be expected to form a larger proportion of eutectic constituents than alloys more remote from this composition (Types 304, 304L, 316 and 308).

This problem is compounded by the fact that both Type 312 and Type 310 tend to exhibit relatively smooth boundary regions along which the low-melting liquid can persist as a continuous film and promote crack formation. Types 304L, 308, and 316 weld pads solidified as primary delta ferrite with a more complex cellular dendritic morphology and produced a smaller proportion of eutectic constituents. For this reason, it is unlikely that continuous films could form along grain and subgrain boundaries, thus reducing the chance of hot crack formation.

Undoubtedly, the segregation of secondary alloying elements and impurity elements, particularly sulfur and phosphorus, have a synergistic effect on promoting or retarding weld hot cracks. Sulfur has frequently been cited as a "bad actor" regarding both hot cracking and

boundary liquation. For this reason, special attention was devoted to this element. In all cases, apparent increases in sulfur concentration were noted at the backfilled regions of cracks tips in both duplex (Type 308 and 312) and austenitic (Type 310) weld pads. However, although the nominal sulfur content of the Type 310 alloy pad was not detectable by microanalysis, sulfur appeared to be present over a 6-micron range within the backfilled region centered on the eutectic ferrite. This indicates that the segregation of sulfur during the final stages of primary austenite solidification is considerable, even in alloys with presumably "safe" levels of this impurity. Phosphorus, which was more easily detected by the electron microprobe, was always observed in increased concentrations within backfilled regions, particularly in the alloys which solidified as primary austenite.

If a small amount of eutectic ferrite forms along the primary austenite subgrain and grain boundaries a portion of the sulfur and phosphorus may be assimilated by the ferrite, thereby reducing the cracking propensity. During solidification as primary delta ferrite, the sulfur and phosphorus are dispersed to a greater degree within the initial solidification product. As a result, less is available for segregation at the solidification boundaries.

Conclusion

Results of the Varestraint test indicated that austenitic stainless steel weldments which solidify as primary delta ferrite and exhibit FN 5-12 in the as-welded microstructure are more resistant to hot cracking than either a wholly-austenitic Type 310 or a highly-ferritic Type 312 weld pad. The coarse grained microstructure of both the Type 310 and Type 312 weldments permit the formation of continuous, low-melting eutectic films along fusion zone grain boundaries. In the presence of sufficient mechanical and/or thermally induced strain, rupture occurs along these liquated boundaries at temperatures below the solidus temperature of the bulk microstructure.

The refined microstructure of the duplex weldments of Type 304L, 316, 308, and 309 creates more boundary area over which low-melting eutectic phases are distributed. As a result, it is unlikely that continuous films could exist. In addition, these alloys contain smaller proportions of chromium and nickel. Thus they would form a smaller amount of eutectic constituents along the solidification boundaries.

The extreme segregation of sulfur and phosphorus into the backfilled cracks of Type 308, 310, and 312 weldments indicates that even small amounts of this element can affect the weldability of the alloy, particularly in alloys which solidify as primary austenite.

Acknowledgments

The authors would like to thank the Alloy Rods Division, Chemetron Corp., a Division of Allegheny Ludlum Corp., for the financial support of this investigation under the auspices of the Chemetron Fellowship. Special thanks are also in order to Brad Petrus who assisted with specimen preparation and metallography.

References

1. Scherer, R.; Riedrich, G.; and Hougardy, H. 1941 (May 6). *Welding rod.*U. S. patent 2,240,672.

2. Borland, J. C., and Youngar, R. N. 1960. Some aspects of cracking in welded Cr-Ni austenitic steels. *British Weld. Jour.* 7 (1): 22-59.

3. Hull, F. C. 1967. Effect of delta ferrite on the hot cracking of stainless steel. *Welding Journal* 46 (9): 399-s to 409-s.

4. Pellini, W. S. 1952. Strain theory of hot tearing. *The Foundry* 80: 125-133.

5. Borland, J. C. 1960. Generalized theory of super-solidus cracking in welds and castings. *British Weld. Jour.* 7: 508-512.

6. Cordea, J. N.; Kammer, P. A.; and Martin, D. C. 1964. Causes of fissuring in nickel-base and stainless steel alloy weld metals. *Welding Journal* 43 (11): 481-s to 491-s.

7. Fredriks, H., and van der Toorn, L. J. 1968. Hot cracking in austenitic stainless steel weld deposits. *British Weld. Jour.* April: 178-182.

8. Gooch, T. G., and Honeycombe, J. 1970. Microcracking in fully austenitic stainless steel weld metal. *Metal Construction and British Weld. Jour.*, Sept.: 375-380.

9. Arata, Y.; Matsuda, F.; and Katayama, F., Solidification crack susceptibility in weld metals of fully austenitic stainless steels (report II). *Trans.* of *JWRI* 5 (1): 19, 105-116.

10. Dahl, W.; Düren, C.; and Müsch, H. 1973. Effect of various alloying elements on the hot cracking susceptibility of austenitic steel during welding. *Stahl und Eisen,* vol. 93: 813-822.

11. Makin, S. M.; Alcock, C. B.; Arkell, D. M., and Pfeil, P. C. L. 1960. Distribution of phosphorus and sulfur in fully austenitic stainless steel welds. *British Weld. Jour.* October: 595-599.

12. Gooch, T. G., and Honeycombe, J. 1975. Microcracking in fully austenitic stainless steel weld metal. *Metal Construction,* March: 146-148.

13. Tumura, H., and Watanabe, T. 1973. Mechanism of liquation cracking in the weld heat-affected zone of austenitic stainless steels. *Trans. JWS* 4 (1): 30-42.

14. Lundin, C. D., and Spond, D. F. 1976. The nature and morphology of fissures in austenitic stainless steel weld metals. *Welding Journal* 55 (11): 356-s to 367-s.

15. Arata, Y.; Matsuda, F.; and Suruwatari, S. 1974. Varestraint test for solidification crack susceptibility in weld metal of austenitic stainless steels. *Trans. JWRI* 3 (1): 79-88.

16. Masumoto, I.; Tamaki, K.; and Kutsuna, M. 1972. Hot cracking of austenitic steel weld metal. *Trans. JWS* 41 (11): 1306-1314.

17. Aström, H.; Loburg, B.; Bengtsson, B.; and Easterling, K. E. 1975. Hot cracking and microsegregation in 18-10 stainless steel welds. *Högskolan I Lulea,* Tuleu: 09, 1-21.

18. Schaeffler, A. L. 1949. Constitution diagram of stainless steel weld metal. *Metal Progress* 56 (5): 680 and 680B.

19. DeLong, W.; Ostrom, G.; and Szumachowski, E. 1956. Measurement and calculation of ferrite in stainless steel weld metal. *Welding Journal* 35 (11): 526-s to 533-s.

20. Gooch, T. G., and Honeycombe, J. 1972. Effect of manganese on cracking and corrosion behavior of fully austenitic stainless steel weld metals. *Metal Construction and British Weld. Jour.,* Dec.: 456-460.

21. Hull, F. C. 1960. Effects of alloying additions on hot cracking of austenitic chromium-nickel stainless steels. *Proceedings, American Society for Testing and Materials,* vol. 60: 667-690.

22. Polgary, S. 1969. The influence of silicon content on cracking in austenitic stainless steel with particular reference to 18Cr—8Ni Steel. *Metal Construction,* Feb.: 93-97.

23. Asakura, S.; Wachi, H.; and Watanabe, K. 1972. The effects of welding conditions on the crack sensitivity of austenitic stainless steel weld metals. *Trans. JWS* 3 (2): 34-44.

24. Goodwin, G. M.; Cole, N. C.; and Slaughter, G. M. 1972. A study of ferrite morphology in austenitic stainless steel weldments. *Welding Journal* 51 (9): 425-s to 429-s.

25. Arata, Y.; Matsuda, F.; and Katayama, S. 1976. Fundamental investigation on solidification behavior of fully austenitic and duplex microstructures and effect of ferrite on microsegregation. *Trans. JWRI* 5 (2): 135-151.

26. Savage, W. F., and Lundin, D. D. 1965. The Varestraint test. *Welding Journal* 44 (10): 433-s to 442-s.

27. Lundin, C. D.; Delong, W. T.; and Spond, D. F. 1975. Ferrite-fissuring relationship in austenitic stainless steel weld metals. *Welding Journal* 54 (8): 241-s to 246-s.

28. Brooks, J. A., and Lambert, F. J., Jr. 1978. The effects of phosphorus, sulfur and ferrite content on weld cracking of Type 309 stainless steel. *Welding Journal* 57 (5): 139-s to 143-s.

29. Lippold, J. C., and Savage, W. F. 1979. Solidification of austenitic stainless steel weldments-part 1, a proposed model. *Welding Journal* 59(12): 362-s to 374-s.